JERZY MAJSZCZYK[1)*], ZBIGNIEW ROSŁANIEC[2)],
DOROTA PIETKIEWICZ[2)], TADEUSZ PAKUŁA[3)]

The phase structure and relaxation phenomena in blends of a poly(ether-ester) elastomer with a liquid crystalline polyester (Vectra)

Summary — Poly(ether-ester) (PEE) Elitel 4450 — liquid crystalline polyester (LCP) Vectra RD 501 blends extruded (L/D = 20, D = 19mm) with a homogenizing head at 225°C, were studied by differential scanning calorimetry (DSC), dynamical mechanical thermal analysis (DMTA), dielectric spectroscopy, and scanning electron microscopy (SEM). The blends exhibited a multiphase microstructure. Two mechanical relaxation temperatures were found to occur, and similarly two glass transition temperatures were recorded by DSC. There is a glass transition in the PTMO soft phase (*ca.* - 60°C) and in Vectra (+ 107°C). For the PBT hard phase (*ca.* +35°C), T_{g2} is weakly pronounced because of the high crystallinity. The blend showed only one m.p., close to the m.p. of the PEE. Three dielectric relaxation processes were found to occur in PEE and three others in Vectra. In the blends, the dielectric spectra are seen to be superimposed. These blends are immiscible in terms of thermodynamics. Vectra modified the molecular mobility of the PEE rigid segments, as evident from nonisothermal crystallization of the PBT hard phase and degree of crystallinity as also from changes of the PTMO content in the soft phase. SEM disclosed either a spherical or a fibrous structure in the blends, depending on Vectra content.

Key words: block copoly(ether-ester), liquid crystalline polyester, polymer blends, Elitel4450—Vectra RD 501 blends, phase structure, physical properties, relaxation phenomena, molecular mobility.

Liquid crystalline polymers (LCP) are conventionally divided into two groups:

(*i*) LCP with mesogenic segments attached to the sides of the main chain and (*ii*) LCP with mesogenic groups incorporated into the main polymer chain.

Group *i* LCP often exhibit a strong electrooptic effect and optical nonlinearity and are applicable in optoelectronic and telecommunication devices [1]. Their viscoelastic properties in the crosslinked state open a possibility of using these materials as a new kind of elastomers with stress-induced liquid crystalline ordering [2].

The excellent mechanical properties and processability, make group *ii* LCP useful as a component of engineering polymer materials [3, 4]. These properties appear because of intermolecular interactions, which make it possible that a fibrous structure appears during processing and orientation. Such a process imparts sort of self-reinforcement to the polymer, which plays the same role as, *e.g.*, whiskers in ceramics and metal-matrix composites [5—7]. This behavior is used in new thermoplastic composites based on conventional plastics and main-chain LCP obtained by blending and compatibilizing. There are, for example: PP/LCP [8], PC/LCP [9], PA/LCP [10], PET/LCP [11], PBT/LCP [12], and PPS/LCP [13] blends in which thermotropic liquid crystalline polyesters are used as LCP.

Block copolymers that contain chain segments distinctly differing in chemical structure and physical properties show a phase-separated microstructure. In poly(ether-ester)s (PEE), the region formed of flexible polyether segments with a low glass transition temperature imparts rubber-like elasticity, whereas rigid polyester micro-domains resulting from specific molecular interaction (*e.g.* crystallization) ensure a sufficiently high mechanical strength [14]. Recently, some compositions of the PEE with other polymers have been manufactured in order to improve mechanical properties (while retaining good flexibility and processability), as blends of PEE with PVC [15], PET [16], PBT [17] and PA [18]. Very interesting elastomers, which exhibit interpenetrating physical network morphologies, have been prepared as blends of PEE with PS or polyurethane [19, 20].

1) Institute of Physics, Technical University of Szczecin, Piastów 17, 70-310 Poland.
2) Institute of Materials Engineering, Technical University of Szczecin.
3) Max Planck Institute for Polymer Research, Mainz, Germany.
*) Author to whom all correspondence should be addressed.

Podstawniki pierścienia fenoksylowego o charakterze elektronoakceptorowym powinny prowadzić do polaryzacji wiązania Ti-O, czyniąc go bardziej jonowym, a tym samym ułatwiać jego rozerwanie. Należy się więc spodziewać odwrotnego wpływu ligandów z podstawnikami elektronodonorowymi, mianowicie zwiększania przez nie kowalencyjnego charakteru wiązania Ti-O. Wiązania kowalencyjne występują w cząsteczce stosowanego często jako kokatalizator $AlMe_3$, a reakcja alkilacji za pomocą tego związku zachodzi poprzez wytworzenie kowalencyjnych mostków M-CH_3-Al (M — metal przejściowy) [10]. Można przypuszczać, że właśnie kowalencyjny charakter wiązań Ti-O-R i Al-Me sprzyja reakcji alkilowania, zwiększając tym samym jej wydajność.

W przedstawionym mechanizmie (schemat Ia) MAO stanowi czynnik alkilujący, który prowadzi do wymiany grup -Cl i -$OC_6H_{5-m}X_m$ na grupy -CH_3 (reakcja Ia.1).

MAO' odgrywa tutaj rolę specyficznego kwasu Lewisa, który prawdopodobnie poprzez akceptorowe oddziaływanie z ligandami CH_3^- związków tytanocenowych powstających w układzie ułatwia reakcję Ia.1 oraz reakcję Ia.2, czyli sprzyja homolitycznemu rozpadowi wiązania Ti-CH_3 w cząsteczce $CpTiMe_3$, a zarazem redukcji Ti(IV) do Ti(III). Analogiczne oddziaływanie występuje prawdopodobnie w reakcji Ia.3, w której powstaje katalitycznie aktywna postać $CpTiMe^+$.

Oczywiście grupy -$OC_6H_{5-m}X_m$ w nowym MAO' będą zmieniać jego właściwości jako kwasu Lewisa. Na obecnym etapie badań nie możemy jeszcze ocenić, jak zmniejszenie, bądź też zwiększenie kwasowości MAO' wpływa na przebieg reakcji Ia.2 i Ia.3. Możemy tylko stwierdzić, że podstawniki X zmieniają liczbę generowanych centrów aktywnych w badanych układach katalitycznych, a tym samym ich aktywność w procesie syndiotaktycznej polimeryzacji styrenu.

Wpływ podstawników X na selektywność polimeryzacji należy wiązać z obecnością w układzie również innych niż $CpTiR^+$ (R — Me lub łańcuch polimeru) postaci katalitycznych. Porównanie mechanizmów polimeryzacji α-olefin i styrenu wobec katalizatorów *ansa*-metalocenowych (czyli zawierających w cząsteczce dwa pierścienie cyklopentadienylowe) wskazuje na konieczność obecności dwóch miejsc koordynacyjnych wokół jonu metalu wykorzystywanych do powstania stereoregularnych poliolefin oraz trzech miejsc koordynacyjnych potrzebnych do uzyskania syndiotaktycznego polistyrenu (polistyren uzyskiwany wobec układów katalitycznych stosowanych w stereoregularnej polimeryzacji α-olefin jest ataktyczny) [7].

W kompleksie aktywnym polimeryzacji olefin dwa miejsca koordynacyjne są kolejno zajmowane przez cząsteczkę olefiny oraz podstawnik alkilowy, który w procesie polimeryzacji migruje do związanej olefiny. W ten sposób rośnie łańcuch polimeru i odtwarza się miejsce koordynacyjne dla następnej cząsteczki monomeru.

W przypadku syndiotaktycznej polimeryzacji styrenu jedno miejsce koordynacyjne w układzie katalitycznym zajęte jest początkowo przez podstawnik alkilowy, później zaś przez cząsteczkę monomeru. Pozostałe dwa miejsca wiążą łańcuch rosnącego polimeru, zapewniając kontrolę nad stereoselektywnością reakcji.

W badanych przez nas układach katalitycznych zarówno wyjściowe kompleksy tytanu, jak i te, które powstają w reakcjach Ia.1 i Ia.2 tworzą wyłącznie postacie katalityczne z dwoma miejscami koordynacyjnymi, a tym samym katalizują reakcję w kierunku ataktycznego PS. Katalizatorami reakcji prowadzącej do ataktycznego PS mogą być również rodniki $CH_3^\bullet$ powstające w reakcji Ia.2 [9]. Postać z trzema miejscami koordynacyjnymi katalizująca powstawanie syndiotaktycznego PS tworzy się dopiero w reakcji Ia.3.

Tak więc, gdy ligand -$OC_6H_{5-m}X_m$ będzie hamował tworzenie jonów $CpTiMe^+$, liczba centrów ataktycznej polimeryzacji styrenu będzie stosunkowo większa, a selektywność procesu w kierunku syndiotaktycznego PS odpowiednio mniejsza. Jest to w pełni obserwowane w badanym przez nas układzie. Należy także stwierdzić, że selektywność polimeryzacji w kierunku syndiotaktycznego PS maleje ze wzrostem temperatury, co można tłumaczyć zarówno zmianami liczby odpowiednich centrów katalitycznych, jak i opisanym w literaturze [11] zmniejszaniem w wyższej temperaturze stereoregulującego działania katalizatora.

LITERATURA.

1. Skupiński W., Niciński K.: *Appl. Organometal. Chem.* 2001, **15**, 635.
2. Ishihara N., Seimyia T., Kuramotoi M., Uoi M.: *Macromolecules* 1986, **19**, 2465.
3. Skupiński W., Wasilewski A.: *J. Organometal. Chem.* 1981, **220**, 39.
4. Fussing I. M. M., Plether D., Whitby R. J.: *J. Organometal. Chem.* 1994, **470**, 109.
5. Skupiński W., Wasilewski A., Woźniewski T., Bazarnik A., Jodłowski M.: *ICRI Annual Report* 1998, 26.
6. Ikai S., Yamashita J., Murakami M., Yano T., Qian Y., Huang J.: *J. Mol. Catal. A; Chem.* 1999, **140**, 115.
7. Ishihara N., Tomotsu N., Newman T. H., Malanga M. T.: *J. Mol. Catal. A; Chem.* 1998, **128**, 167.
8. Grassi A., Zambelli A.: *Organometallics* 1996, **15**, 480.
9. Po R., Cardi N.: *Prog. Polym. Sci.* 1996, **21**, 47.
10. Tsirkov N. M., Matkovskij P. E., Dyiakovskii F. S.: „Polimerizaciya na kompleksnykh metallo-organicheskikh katalizatorakh", wyd. Khimiya, Moskwa 1976, str. 37.
11. Chien J. C. W., Salajka Z.: *J. Polym. Sci. A; Polym. Chem.* 1991, **29**, 1253.

Otrzymano 10 X 2000 r.

The present work examines the molecular dynamics and phase structure of the system which contains a multiblock poly(ether-ester) (PEE) and a main-chain liquid crystalline polyester (Vectra, LCP) by such experimental techniques as dielectric spectroscopy, thermal analysis (DSC), dynamic mechanical thermoanalysis (DMTA) and scanning electron microscopy (SEM).

EXPERIMENTAL

Materials

The PEE (I) used in this work: Elitel 4450, produced by the Elana SA (Toruń, Poland); which consists of 50 wt% of rigid crystalline poly(tetramethylene terephthalate) segments and 50 wt% of flexible amorphous poly(tetramethylene oxide) segments. The melting and crystallization characteristics of the PEE as well as its rheological properties have been described elsewhere [14, 21]. The liquid-crystalline polyester (II), trade name

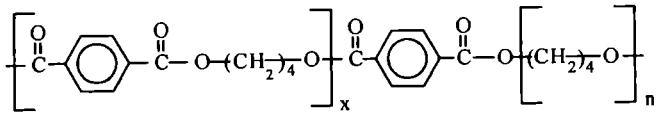

(I)

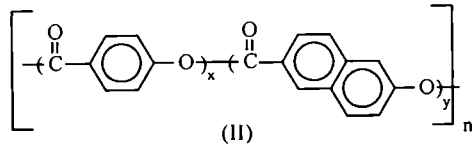

(II)

Vectra grade RD 501, was supplied by the Hoechst Cellanese. The melting point of this Vectra RD 501 is about 220°C, much lower than, *e.g.*, for Vectra 950. These materials were first dried in a vacuum oven at 100°C for 24 h to remove absorbed water and then used as components to make the investigated blends.

Blending and preparation of samples

Dried pellets of the polymer components were mixed and blended in the molten state in a laboratory extruder (L/D = 20; D = 19 mm) equipped with a homogenizing head (L/D = 2) at temperatures of 190, 190, 225, 210°C (in the corresponding number of zones) and then granulated. The samples for DSC and dielectrical measurements were prepared in the form of films by compression molding between PTFE plates. This process was started at 230°C and the samples were placed in the press for 2 min at 180°C and then quenched in cold water. The films for dielectric measurements about 50 μm thick, were dried in vacuum, and furnished with circular gold electrodes 2 cm in diameter by the vacuum sputtering technique. The samples for dynamic mechanical analysis and for scanning electron microscope tests were prepared by injection molding at 235°C and 35 MPa.

Molecular mobility

Dielectric spectroscopy was applied to study the molecular dynamics of the PEE, Vectra and their blends. These measurements gives the complex dielectric permittivity ε* as a function of frequency and temperature

$$\varepsilon^* = \varepsilon' - i\,\varepsilon'' \tag{1}$$

where ε′ *is the real part of the permittivity (or dielectric constant) and* ε″ *is the imaginary part (or dielectric loss) and* $i = (-1)^{1/2}$. In polar dielectrics the response of the sample to electric field oscillation has a relaxational character, *i.e.* the ε″(ω) or ε″(T) relationships show one or more maxima. In order to describe the relaxational behavior of polymeric material, two different equations are commonly used [22]. The one is for an Arrhenius-type dependence as observed for the relaxations corresponding to small scale motion (denoted as β- or γ-processes)

$$f_{max} = f_{\infty} \exp\left(\frac{-E_a}{kT}\right) \tag{2}$$

where f_{max} *is the frequency related to maximum in* ε″, f_{∞} *is the pre-exponential factor,* E_a *is the activation energy,* k — *the Boltzmann constant and* T — *the absolute temperature.*

The other describes the temperature dependence observed for the relaxation associated with the motions appearing at the glass transition temperature (usually denoted as α-process) and it is called the Vogel-Fulcher equation

$$\log(f_{max}) = B - A/(T - T_0) \tag{3}$$

where A, B *and* T_0 *are constants characteristic for the system.*

When the investigated material reveals DC-conductivity, which is seen in the region of high temperatures and low frequencies in the form of rough increase in ε″-values, it is difficult to distinguish the maximum value of ε″ ; the α-relaxation is seen only at higher frequencies, while at lower it is terminated by conductivity relaxation. In such a case an electric modulus $M^* = 1/\varepsilon^*$ can be applied to the analysis of experimental data [23]

$$M^* = \varepsilon'/\left[(\varepsilon')^2 + (\varepsilon'')^2\right] - i\varepsilon''/\left[(\varepsilon')^2 + (\varepsilon'')^2\right] = M' - iM'' \tag{4}$$

Dielectric measurements were carried out with a broadband device of Solatron Schlumberger Frequency Response Analyzer 1260. Temperature was controlled to within 0.1 K by the Novocontrol System using nitrogen gas supplied directly to the sample chamber.

Phase behavior study

Differential scanning calorimetry (DSC), dynamical mechanical thermal analysis (DMTA) and scanning electron microscopy (SEM) were used to study molecular interactions and phase structure in the materials mentioned above.

Molecular interactions in the system containing two or more polymers determine the thermodynamic miscibility or phase separation. For an amorphous/semicrystalline polymer blend, molecular interactions and the miscibility can be estimated on the basis of the glass transition temperature T_g and depression of the melting point T_m. The glass transition temperature of a two-component blend can be described by the Kwei equation [24]

$$T_g = (w_1 T_{g1} + k w_2 T_{g2}) / (w_1 + k w_2) + q w_1 w_2 \quad (5)$$

where: *w_1 and w_2 are the weight fractions, T_{g1} and T_{g2} — the glass transition temperatures of components 1 and 2, respectively; k and q are the parameters used to characterize intermolecular interactions.* The degree of soft phase separation, W_{fs} for copoly(ether-ester) can be calculated by the following equation [24]:

$$W_{fs} = \frac{1}{w_s} \cdot \frac{\Delta Cp^{obs}}{\Delta Cp_s} \quad (6)$$

where: *ΔCp^{obs} is the observed heat capacity of the copolymer or blend and ΔCp_s is the heat capacity of the polyether used as a flexible segment.*

Thermal properties, such as heat capacity, heat of fusion and temperatures T_g, T_c and T_m, were measured with a Perkin-Elmer DSC-7 and a Mettler microcalorimeter in a triple cycle of heating-cooling-heating, within the temperature range of -120°C to 250°C and at a scanning rate of 10°C/min. Glass transition temperatures of the blends were determined by the middle point of the heat capacity change ($\frac{1}{2}\Delta Cp$); the melting point T_m and the crystallization temperature T_c were determined as the temperatures of extremum exothermic or endothermic effect.

DMTA measurements were carried out by using a Polymer Laboratories MKK II instrument at a frequency of 1 Hz and a heating rate of 3°C/min. The storage modulus E', loss modulus E'' and tan δ were determined as a function of temperature, whereas the temperature of maximum of E'' (*i.e.* the α-relaxation) was taken as the glass transition temperature.

For microscopic observations of the polymer structure a JEOL JSM 6100 scanning electron microscope was used.

RESULTS AND DISCUSSION

The materials studied in this work are blends of the copoly(ester-ether) (PEE) containing 50 weight % of poly(oxytetramethylene) and 50% poly(butylene terephthalate) segments with the liquid crystalline polyester Vectra, within 0 to 50 weight % of the LCP in the system. The disparate molecular mobilities of the flexible polyether and the stiff polyester segments in the PEE as well as the stiff mesogenic chain fragments in the LCP reflect on the dynamics of the relaxation processes and phase separation. In addition, unequivalent interaction between the block copolymer segments and the blend components affect physical properties of the system.

Thermal properties

Results of DSC and DMTA thermal and thermo-mechanical studies are presented in Table 1 and in Figs. 1—4. The DSC thermograms show two glass temperatures to be characteristic for the PEE: the lower (T_{g1}) at about -60°C and the higher (T_{g2}) at +35°C. These temperatures are related to the soft phase containing many PTMO segments, and to semicrystalline hard phase created by the PBT segments, respectively. The melting point of the last phase is T_m = 192°C. The LCP Vectra has one glass temperature, T_g = 107°C and a melting point with a small endothermal maximum at T_m = 229°C, which corresponds to the transition from the crystalline to the nematic LC phase. The glass temperatures of the PEE/LCP blends are only slightly related on the blend composition (see Figs. 1 and 2; Table 1). The higher

T a b l e 1. Results of DSC and DMTA investigations on PEE/LCP Vectra blends

	Sample Number								
	1	2	3	4	5	6	7	8	9
PEE/LCP, wt %	100/0	95/5	90/10	85/15	80/20	75/25	70/30	50/50	0/100
T_{g1} (PEE), °C	-62	-63	-61	-66.5	-61	-62	-60.5	-58	—
ΔC_{p1}, J/g · °C	0.19	0.22	0.25	0.18	0.22	0.17	0.23	0.18	—
T_{g2} (PEE), °C	54	51	52	53	52	56	51	55.5	—
T_{g3} (LCP), °C	—	—	—	—	—	—	—	—	107
T_m, °C	192	194	193.5	194	193	194	193.5	192	221.5
ΔH_m, J/g	34.5	33.1	32.4	29.9	29.1	26.3	26.6	18.5	2.8
T_c, °C	155	169	166	167	163	167	166	160.5	177
ΔH_c, J/g	33.6	32.1	32.3	30.4	28.8	26.1	25.7	18.8	2.8
T_1, °C	-45.5	-49.0	-48.4	-48.1	-47.7	-45.6	-44.8	-46.4	—
T_2, °C	—	104.5	104.8	105.8	107.2	107.2	107.2	106.4	107.2

Results of DSC investigations: T_g — glass temperature, ΔC_{p1} — specific heat change at T_g, T_m — melting temperature, ΔH_m — melting enthalpy, T_c — temperature of crystallization, ΔH_c — heat of crystallization; results of DMTA investigation: T_1, T_2 — relaxation temperatures.

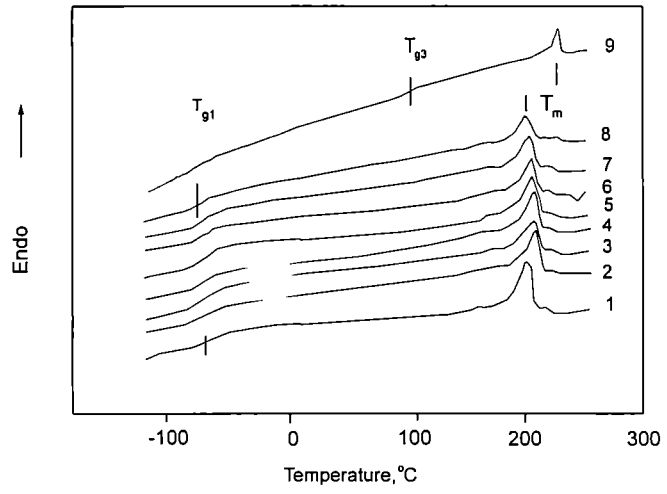

Fig. 1. DSC thermograms, glass transition temperatures T_{g1},T_{g3} and melting temperatures T_m for PEE / Vectra blends (second heating run; heating rate, 10°C/min) (in each figure for curve number see Table 1)

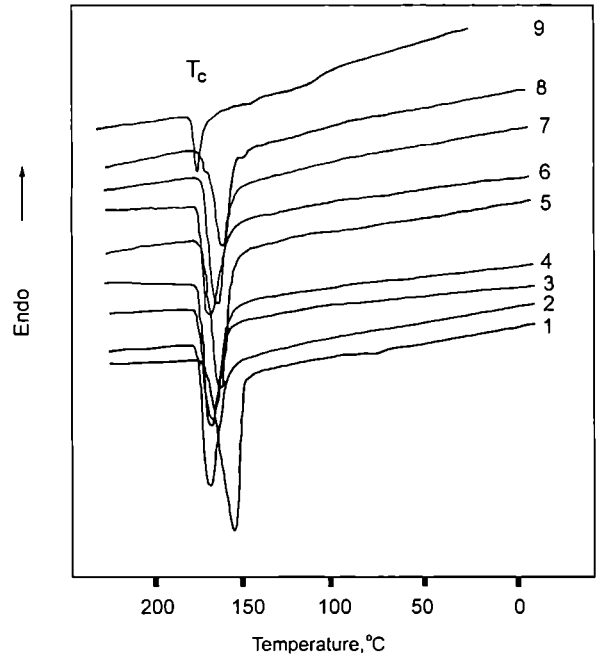

Fig. 2. DSC thermograms and crystallization endotherms of PEE/Vectra blends (cooling rate: 10°C/min)

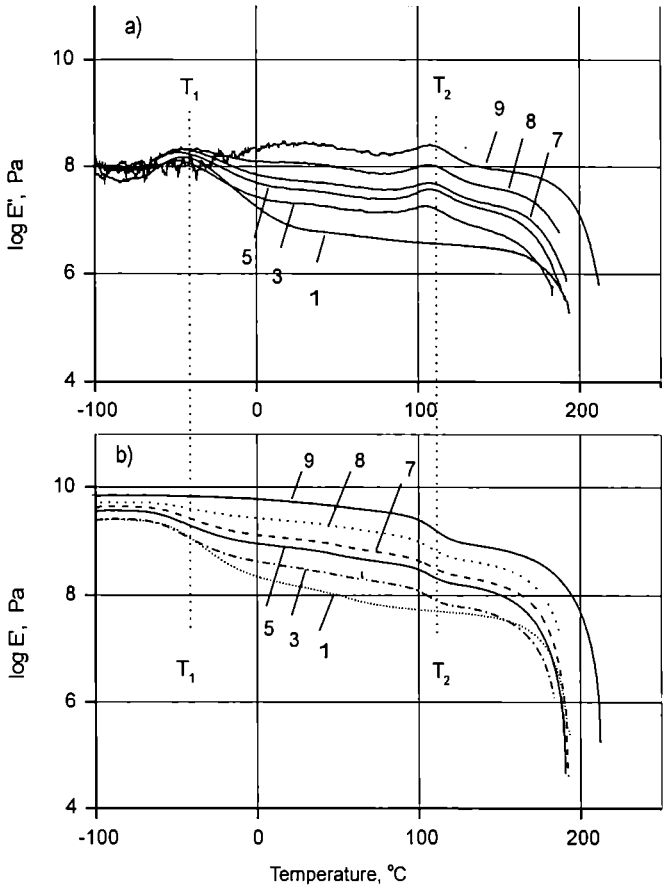

Fig. 3. (a) Storage modulus (from DMTA) of PEE /Vectra blends versus temperature. T_1, T_2 — temperatures of relaxation processes corresponding to glass transitions (see Figs. 1 and 4); (b) loss modulus of PEE/ Vectra blends versus temperature (numbers on curves correspond to sample numbers in Table 1)

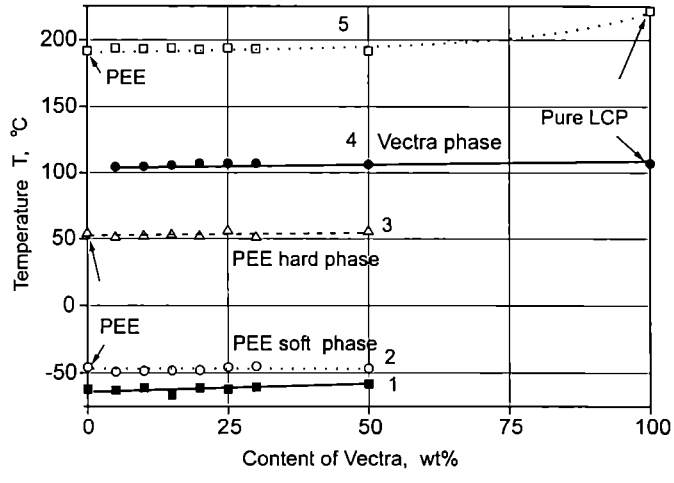

Fig. 4. Some characteristic temperatures in relation to composition of PEE /Vectra blends; 1 — T_{g1} (DSC), 2 — T_1 (DMTA), 3 — T_{g2} (DSC), 4 — T_2 (DMTA) and 5 — T_m (DSC)

glass transition effect (at T_{g2}) is poorly distinguished in the DSC thermograms (except for first runs); therefore the values presented in Table 1 are taken from the first runs. Two transitions at T_1 and T_2, corresponding with T_{g1} and T_{g3}, are clearly seen in the DMTA plots (Fig. 3a, b; Table 1). The transition at T_{g2} (for the PBT hard phase, *ca.* +35°C) is weakly pronounced because of its high crystallinity. The DSC and DMTA results confirm the existence of three different glass transitions: T_{g1}, T_{g2} and T_{g3} in the blends, related to their components. The glass temperatures depend only slightly on the blend composition (Fig. 4). These facts suggest that PEE and LCP Vectra produce thermodynamically immiscible systems with a heterophase structure (which does not mean that there are no interactions between the components). The irregular distribution of T_{g1} values in the blends is correlated with a similar distribution of T_m. For semicrystalli-

ne component T_m increases on account of small content of the second (soft) component of the blend; the above can result from an influence of the LCP onto PEE during a non-isothermal crystallization process. H. Yan *et al.* [25] have found a similar behavior in the blend of LCP and poly(butylene terephthalate) (PBT); the result is the rise of the melting temperature and the increase in the degree of hard segment crystallinity. In our case, the increment of the crystallinity degree of the PBT-phase (*cf.* Fig. 5a) brings about a microphase balance change between PBT and PTMO in the PEE matrix. As a result, the polyether (amorphous) phase composition changes toward a greater contribution of the PTMO (Fig. 5b). Such a result could be explained by the increment of the PBT-chains during the crystallization in contact with Vectra.

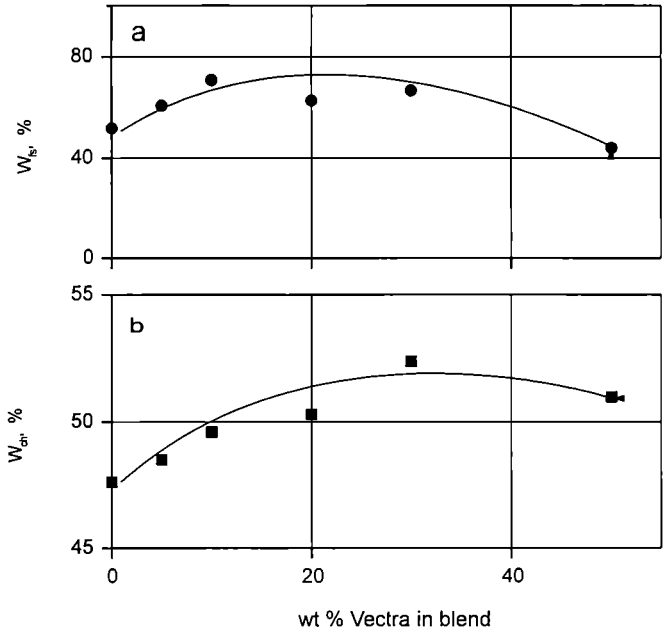

Fig. 5. a) Correlation between PTMO segments content in soft phase and content of Vectra in PEE /Vectra blends, b) degree of crystallinity W_{CH} of PBT phase in PEE/Vectra blends as a function of Vectra content

Dielectric relaxation

For pure PEE, pure LCP and blends containing 5%, 10%, 25% and 50% of LCP, complex dielectric permittivity ε* was measured as a function of the frequency and temperature. Figures 6 and 7 present dielectric loss ε" in relation to temperature for the PEE and LCP Vectra, at some selected frequencies; arrows point to particular relaxation regions. The results obtained for pure components are in good agreement with these published by Z. Rosłaniec *et al.* [26] for the PEE and by A. Boersma *et al.* [27] for Vectra. In Fig. 8 the isochronal (*i.e.* at constant frequency) dependence ε"(*T*) is presented for the PEE/LCP blends. These spectra of the blends are seen to be simple superpositions of the spectra of pure components. These results allowed to construct a relaxation plot showing a frequency related to maximum value of the ε" *versus* reciprocal temperature $1/T$ (Fig. 9). The curves for pure LCP Vectra and for Vectra in blends overlap each other, whereas those for PEE are slightly shifted, having almost the same values of the activation energy E_a. These facts are one more confirmation of the heterophase structure of the blends and show the influence of the LCP Vectra on the molecular mobility of the PEE. Results of dielectric measurements for each sample were phenomenologically analyzed by means of equations (2) and (3). The resulting parameters are collected in Table 2. The $\alpha_1$and α_2 processes observed in the PEE (see Fig. 6) are related to glass transitions of the soft and the hard phases, respectively; the second is terminated by DC-conductivity of the PEE and no calculation is possible to perform.

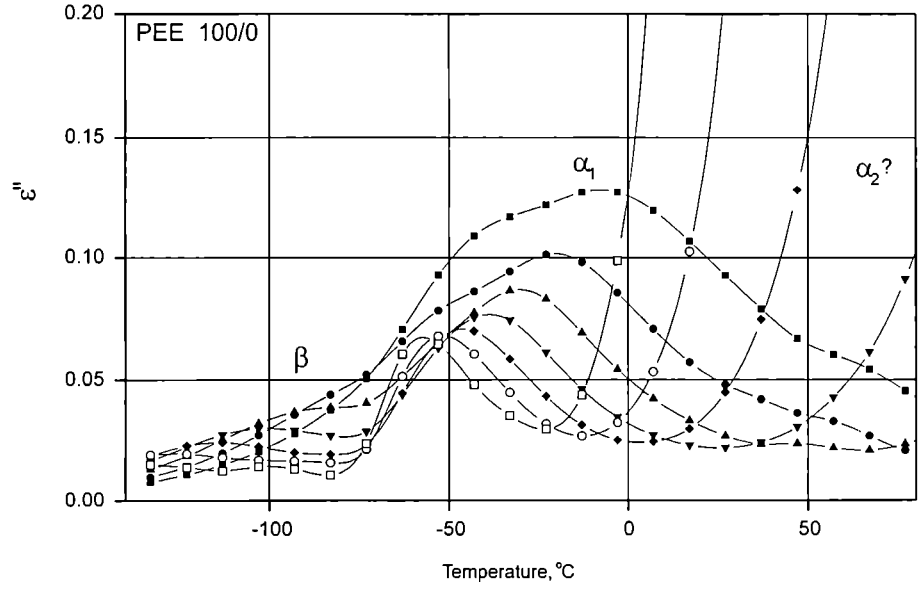

Fig. 6. Temperature dependence of dielectric loss ε" in PEE at some selected frequencies: □ — 1 Hz, ○ — 10 Hz, ♦ — 100 Hz, ▼ — 1 kHz, ▲ — 10 kHz, • — 100 kHz, ■ — 1 MHz. α_2?— note that α_2-process is masked by DC-conductivity in the soft phase

T a b l e 2. Fitting parameters to dielectric measurement data in equations (2) and (3)

	Sample number					
	1	2	3	6	8	9 (pure LCP)
PEE/LCP, wt %	100/0	95/5	90/10	75/25	50/50	0/100
α-relaxation, B	14.2	14.4	16.3	18.2	19.2	18.7
α-relaxation, A, K	1002	1022	1210	1745	1944	142
α-relaxation, T_0, K	144.7	147	131.5	127.3	117.4	380
β-relaxation, E_a, kJ/mol	35	34	36	36	33	102
γ-relaxation, E_a, kJ/mol	—	—	—	—	—	34

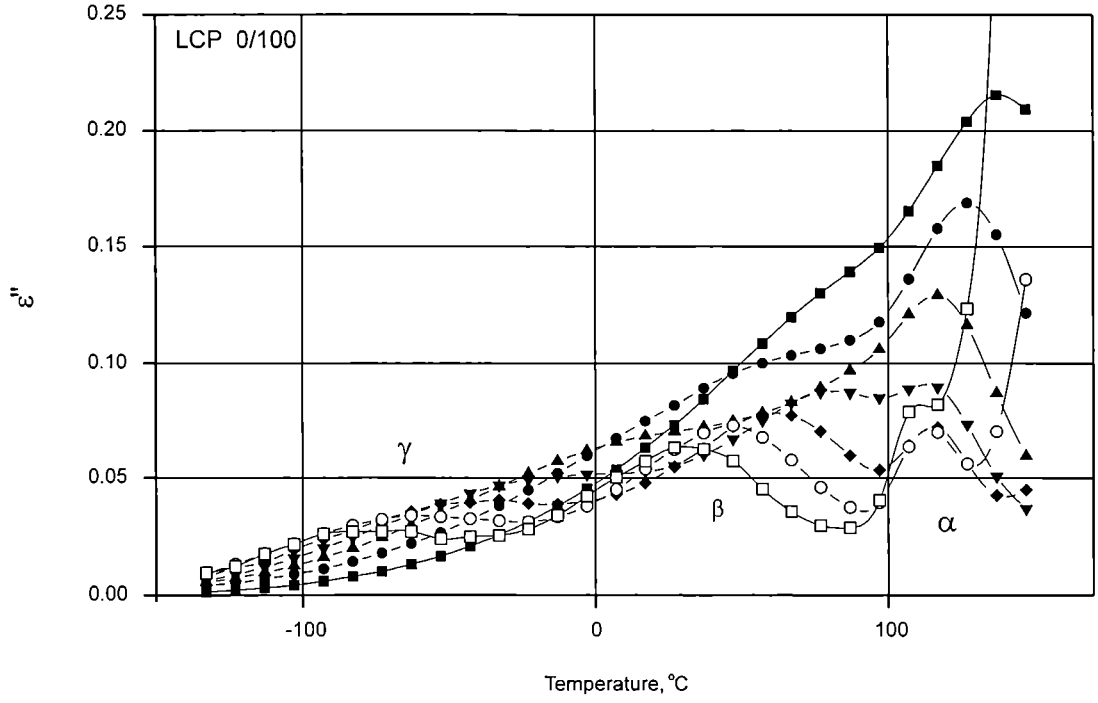

Fig. 7. Temperature dependence of dielectric loss ε" in LCP Vectra (for symbols see Fig. 6)

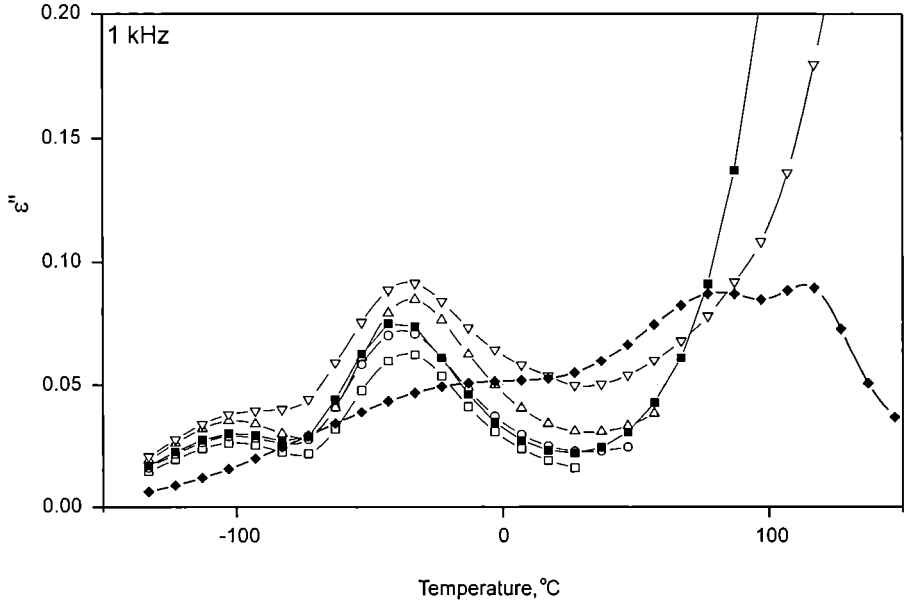

Fig. 8. Temperature dependence of dielectric loss ε" in PEE/ LCP blends at 1 kHz. PEE / LCP ratio: ■ — 100/0, ∇ — 95/5, Δ — 90/10, ○ — 75/25, □ — 55/50, ♦ — 0/100

In order to analyze of the AC-conductance, which is clearly expressed at low frequencies and high temperatures in the form of anomalous rise of ε" (see Figs 6—8), the presentation of the results by electric moduli according to Equation (4) was used. An example for the PEE is presented in Fig. 10a. A symmetric shape of the M"*(f)*

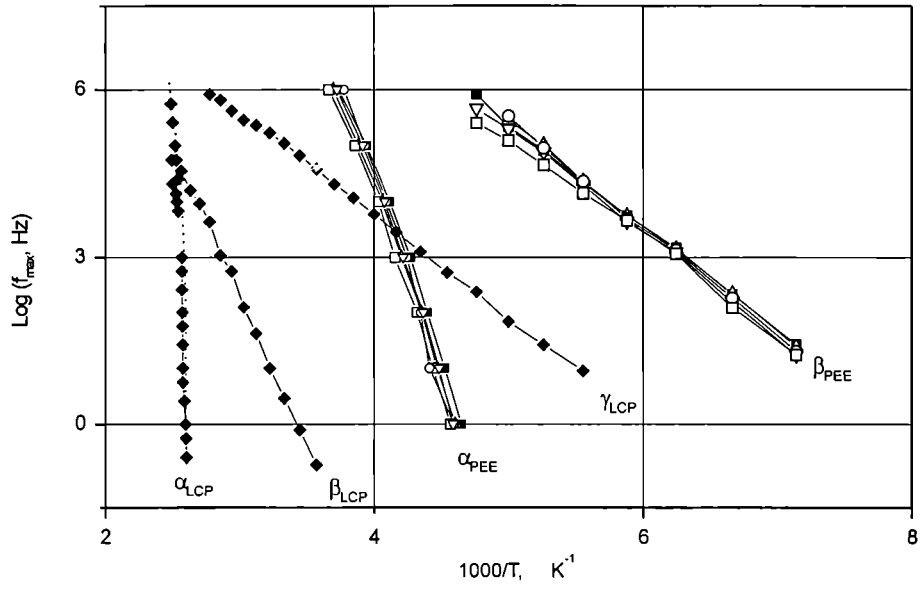

Fig. 9. Dielectric relaxation map for PEE/LCP blends; symbols for PEE/LCP ratio as in Fig. 8. Plots for pure LCP Vectra and Vectra in blends are almost identical

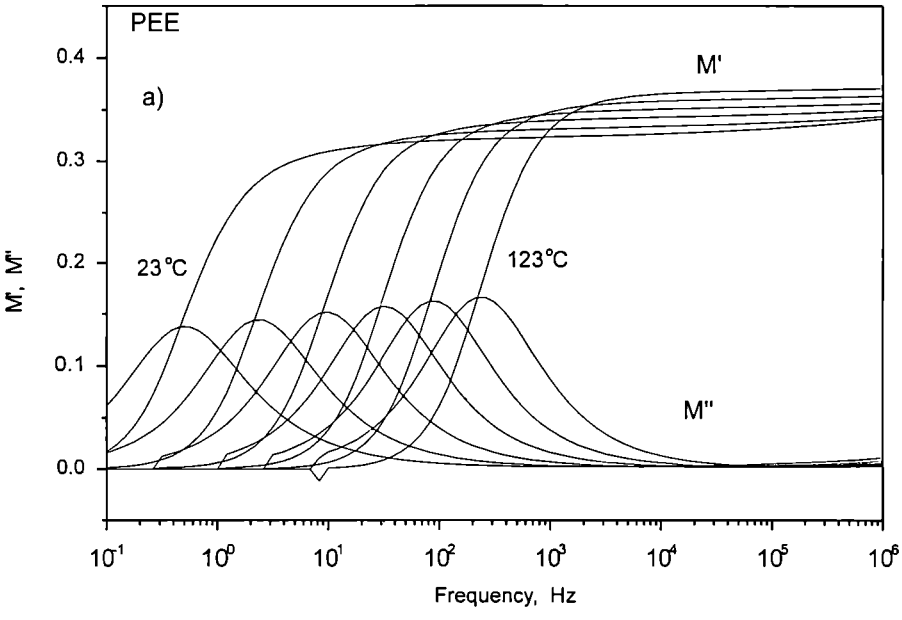

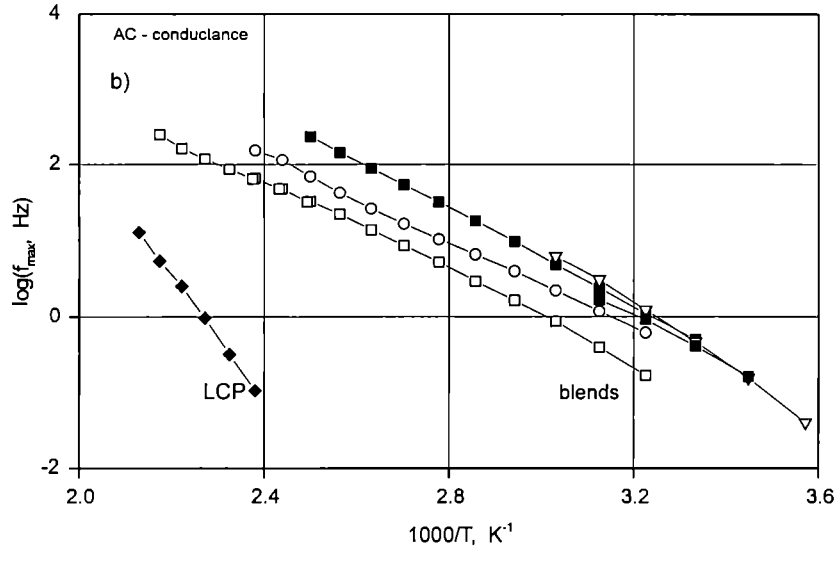

Fig. 10. (a) Dielectric loss modulus M" (see Eq. 5) of PEE versus frequency at selected temperatures, (b) log plot of frequency corresponding to maximal value of M" versus reciprocal temperature; values of activation energies of DC-conductivity are within 60 ± 2 kJ/mol for each blend, excluded pure Vectra, (176 kJ/mol). PEE/LCP ratio symbols are the same as in Fig. 8

curves indicates the Debye-like character of the charge carriers relaxation process observed. On the basis of these recalculated data, a new relaxation plot was produced (Fig. 10 b). Figure10b shows the DC-conductance of the PEE to play a dominant role in the PEE/LCP blends; its activation energies are equal to 60 ± 2 kJ/mol, almost independently from the LCP Vectra contents. It could be interpreted that the soft, more conducting, amorphous PEE-phase is the continuous phase, even at 50% content of the LCP Vectra; it is also the proof for the phase separation occuring in these blends.

Phase structure

Phase structure of the PEE/Vectra blends studied by scanning electron microscopy (SEM) indicates the existence of two phases (Fig. 11). At low LCP concentration in the blend, small microspheres of the Vectra are located in the PEE matrix (Fig. 11a). At concentrations higher than 20 wt% of Vectra, fibrous structure appears, which is responsible for the improvement of mechanical properties of the blend (see Table 3). Fig. 11c presents complex fibrous structure of the blend, where PEE fibers appear also inside the LCP fibers. Such fibrous structure was observed in other LCP blends, *e.g.*, in PBT/LCP and PET/PHB systems [28]. The system does not exhibit any symptoms of interphase adhesion, so it may be considered as the incompatible heterophase blend. It is noteworthy that there are three phases evident in the DSC and DMTA results. This fact could be explained by considering the PEE to undergo microphase separation during non-isothermal crystallization of the PBT segments, a fact not detected in the SEM images. This process also plays role as an initiator for macrophase separation in the PEE/Vectra system (thermotropic properties of the Vectra also affect the microphase structure of PBT segments in PEE, as mentioned above).

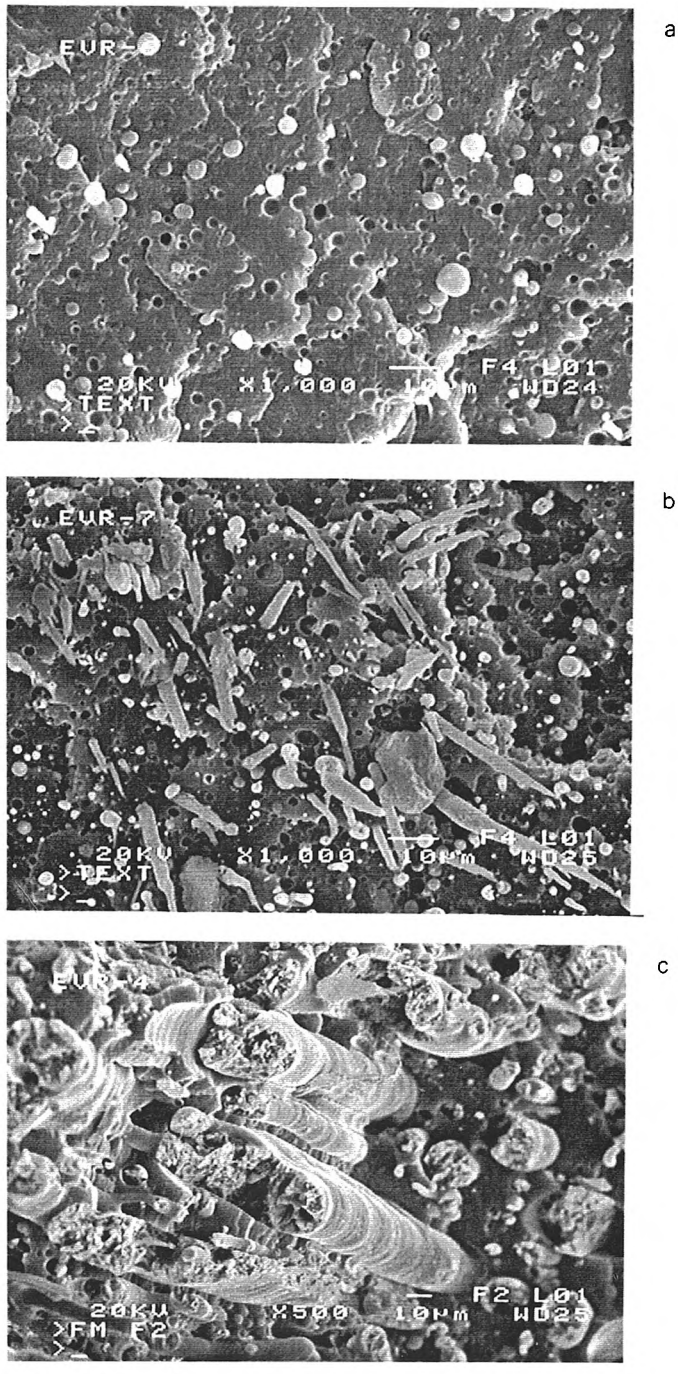

Fig. 11. Scanning electron micrographs of PEE/Vectra blends. PEE/LCP ratio (wt%): (a) 85/15, (b) 75/25, (c) 50/50

T a b l e 3. Basic physical property data on the PEE/LCP blends

	Sample Number								
	1	2	3	4	5	6	7	8	9
PEE/LCP, wt %	100/0	95/5	90/10	85/15	80/20	75/25	70/30	50/50	0/100
T_1, °C	196—202	200—210	204—223	200—230	204—220	200—230	210—233	207—239	228—236
ρ, 10^3 kg/m^3	1.16	1.12	1.18	1.20	1.22	1.21	1.23	1.26	1.34
MFR, g/10 min	55.3*	44.6*	25.3	24.8	24.4	17.3	11.0	65.7*	40.7*
H, D-scale	44	47	50	51	51	55	57	65	81
σ_s, MPa	11.3	15.0	16.7	16.4	20.3	22.3	32.8	28.9	88.0
σ_r, MPa	21.7	22.2	18.8	11.4	6.8	10.5	15.1	28.9	86.9
E, MPa	115	104	387	166	954	323	1744	2681	4303
ε, %	550	826	380	430	34	30	6	3	9

T_1 — melting temperature by Boëtius hot-stage, ρ — density, *MFR* — Melt Flow Rate at 205°C and * 225°C, *H* — hardness by Shore D, σ_s — stress at plasticity limit, σ_r — breaking stress, *E* — Young modulus, ε — elongation at break.

CONCLUSIONS

1. The PEE/Vectra blends obtained from the melt exhibit either micro- or macro-heterophase structure.

2. The thermotropic properties of the Vectra affect the non-isothermal crystallization process of the PBT segments. This influence manifests itself by changes in the microphase structure of the PEE.

3. The fibrous structure of the blends is the cause of *in situ* reinforcement of the PEE matrix. This is one of possible ways to prepare semi-elastic polymeric composites.

4. Electrical properties of the blends are determined mainly by the properties of the PEE matrix and are only slightly related to the LCP contents.

5. The PEE/LCP blends of the PEE Elitel 4450 and Vectra grade RD 501 are promising engineering materials for many applications; some basic physical properties are listed in Table 3.

ACKNOWLEDGMENTS

The Polish State Committee for Scientific Research is gratefully acknowledged for the support of this investigation by Grant No. KBN-GW/RKH 1999 (J. M.) and Grant No. 3T09B 070 14 (Z. R. and D. P.).

Published by the kind permission of Koecht—Celanese S.A., Poland.

REFERENCES

1. Chilton J. A., Goosey M. T.: "Special Polymers for Electronics and Optoelectronics", Chapman & Hall, London 1995, 256.
2. Weilepp J., Zanna J. J., Assfalg N., Stein P., Hillion L., Mauzak M., Filkenman H., Brand H. R., Martinoty P.: *Macromolecules* 1999, **32**, 4566.
3. Carfagna C.: "Liquid Crystalline Polymers", Pergamon Press, Oxford 1994.
4. Domininghaus H.: "Plastics for Engineers", Hansen Publ., Munich 1993.
5. Fakirov S. (Ed.): "Oriented Polymeric Materials", Huthing—Wepf, Heidelberg 1996.
6. Zheng L., Jin Y., Li P.: *Compos. Sci. Technol.* 1997, **57**, 463.
7. Avella M., Martuselli E., Raimo M., Partch R., Ganolli S. G., Pasucci B.: *J. Mater. Sci.* 1997, **32**, 2411.
8. Kozłowski M., La Mantia F. P.: *J. Appl. Polym. Sci.* 1997, **66**, 960.
9. Römer M., Neupauer A.: *Kunststoffe* 1996, **86**, 1310.
10. Kirswanaswamy R. K., Bin Wadud S. E., Baird D. G.: *Polymer* 1999, **40**, 701.
11. Carpaneto L., Lesage G., Pisino R., Trefiletti V.: *Polymer* 1999, **40**, 1781.
12. Yan, H., Xu, J., Mai, K., Zeng, H.: *Polymer* 1999, **40**, 4865.
13. Gopakumar T. C., Ponrathnam S., Lele A., Rajan C. R., Fradet A.: *Polymer* 1999, **40**, 357.
14. Pożdżał R., Rosłaniec Z.: *Kautch. Gummi Kunst.* 1999, **52**, 656.
15. Kwak S. Y., Nakajima N.: *Macromolecules* 1996, **29**, 3521.
16. Skafidas D. S., Kalfoglou N.: *Polymer* 1997, **38**, 1057.
17. Kallager K. P., Zhang X., Runt J. P., Huynhaba G., Lin J. S.: *Macromolecules* 1993, **26**, 588.
18. Koulouri E. G., Scourlis E. C., Kallitsis J. K.: *Polymer* 1999, **40**, 4887.
19. Veenstra H., Van Dam J., Posthuma de Boer A.: *Polymer* 1999, **40**, 1119.
20. Rosłaniec Z.: *Polymer* 1993, **34**, 359.
21. Rosłaniec Z.: *Polymer* 1993, **34**, 1249.
22. Runt J. P., Fitzgerald J. J.; "Dielectric Spectroscopy of Polymeric Materials", American Chem. Soc., Washington, DC 1997, 86.
23. Moynihan C. T.; *J. Non-Cryst. Solids* 1996, **203**, 359
24. Kwei T. K.: *J. Polym. Sci; Polym. Lett.* 1984, **22**, 307.
25. Yan H., Xu J., Mai K., Zeng H.: *Polymer* 1999, **40**, 4865.
26. Rosłaniec Z., Ezquerra T., Baltá-Calleja F.: *Colloid Polym. Sci.* 1995, **273**, 58.
27. Boersma A., van Turnhout J., Wübbenhorst M.: *Macromolecules* 1998, **31**, 7453.
28. Kang T. K., Kim Y., Ha C. H.-S.: *J. Appl. Polym. Sci.* 1999, **74**, 1797.

Received 14 I 2000.
Revised version 19 II 2001.